

BSc Thesis
Applied Mathematics & Applied Physics

The effect of an external
magnetic field on an
antiferromagnetic
two-dimensional square Ising
model with anisotropic nearest
neighbour interaction

W.F.G. Rorink

Supervisors:

Prof. Dr. Ir. H.J.W. Zandvliet (TNW-PIN)

Prof. Dr. R.J. Boucherie (EEMCS-SOR)

Reference members:

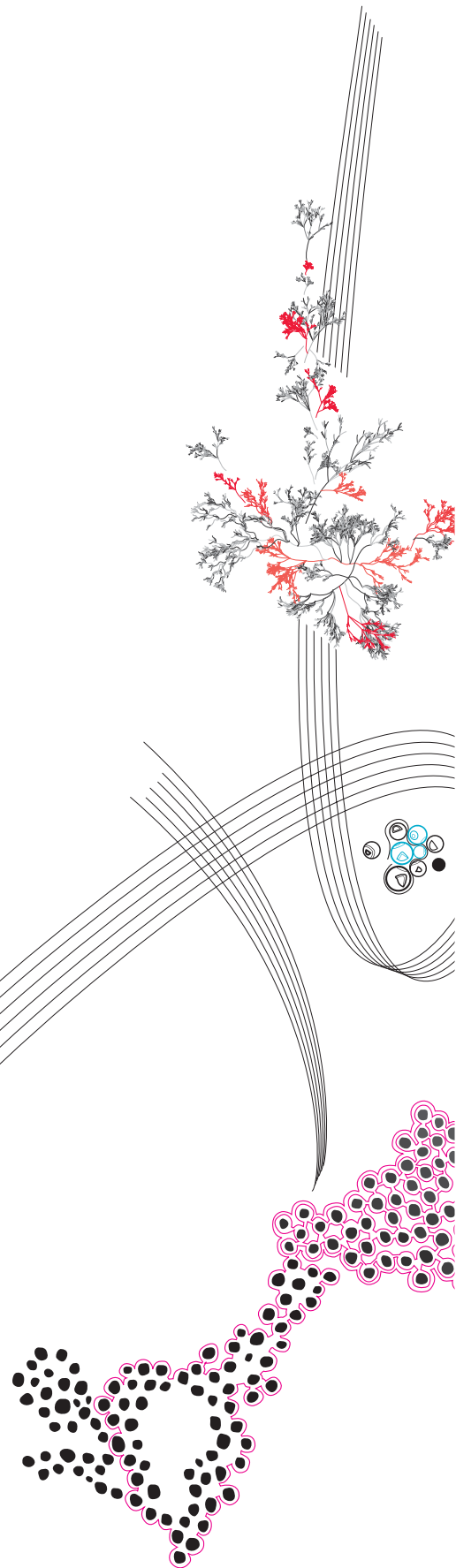
prof.dr.ir. B.J. Geurts (EEMCS-MMS)

prof.dr.ir. H.L. Offerhaus (TNW-OS)

June 25, 2024

Department of Applied Physics
Faculty of Science and Technology

Department of Applied Mathematics
Faculty of Electrical Engineering,
Mathematics and Computer Science



Preface

Before you lies the bachelor's thesis on "The effect of an external magnetic field on an antiferromagnetic two-dimensional square Ising model with anisotropic nearest neighbour interaction". It has been written as part of the graduation requirements for the Applied Mathematics (AM) and Applied Physics (AP) programmes at the University of Twente. This thesis marks the finalisation of my three years of study with the double degree programme of AM&AP.

In this report, I will attempt to find a closed analytic solution for the critical temperature of the order-disorder phase transition for a two-dimensional antiferromagnetic square Ising lattice with anisotropic nearest neighbour interactions and an external magnetic field. The influences of a magnetic field on phase transitions, or phase transitions in general are interesting because they are omnipresent in nature yet their mathematical descriptions are often lacking due to their complexity. With my research, I hope to describe a closed expression for a well-known problem within the field of statistical mechanics with a promising analytical approach. With this derivation, I would like to find results and insights that are both mathematically rigorous and physically meaningful.

These results could provide us with more insight into the complexity of phase transitions. Because the Ising model serves as a cornerstone in the field of statistical physics, solving it under various conditions, like an external magnetic field, could help with the theoretical foundation of condensed matter physics and with practical implications in material science or magnetism. Furthermore, the Ising model finds application in fields beyond physics like economics, neuroscience, mathematics and even certain parts of social science. If we have more understanding of the Ising model with certain constraints this could prove the model useful for more applications for physics but also beyond.

I would like to thank my supervisors, Harold and Richard, for their guidance and support during my research. Harold showed great interest in the topic and was always available for questions or discussions about every part of the research. Even during his vacation period, he made sure he was available for questions or feedback. Richard always made sure that what was written down was rigorous and well-substantiated. He questioned the assumptions and steps made and assured the article would have the desired justified result and well-defined structure. I also would like to thank the people in the research department Physics of Interfaces and Nanomaterials (PIN) for their hospitality during my project. For example: an office space, the reminders to take a break and the many conversations and fun activities.

Finally, I want to thank my family and friends for being there for me during this project, and my entire studies so far, directly or indirectly. I want to thank Alwin, Danny and Lars explicitly for their friendship, support and help with discussions and derivations. And for you, my reader: I hope you enjoy your reading.

Wout Rorink
Enschede, June 2024

Contents

1	Introduction	1
2	Anisotropic Derivation	2
2.1	Boundary formation	3
2.2	Kink formation	4
2.3	Partition function	5
2.4	Absolute convergence of the infinite series	6
2.5	Phase Boundary Equation	8
2.6	Phase diagrams	9
2.6.1	Ferromagnetic alignment condition	10
2.6.2	Isotropic phase diagram	10
2.6.3	Anisotropic phase diagrams	11
2.7	Vanishing magnetic field	13
2.8	General Results	15
3	Discussion and conclusion	17
3.1	Ground state of the boundary	17
3.2	Decoupling in the phase diagrams	19
3.3	Correctness of the partition function	20
3.4	Conclusion	20
3.5	Outlook	21
4	References	22
A	Isotropic Derivation	24
A.1	Boundary and kink formation	24
A.2	Partition function	25
A.3	Absolute convergence of the infinite series	27
A.4	Phase Boundary Equation	28
A.5	Phase diagram	29
A.6	Vanishing magnetic field	30
B	Root test	31

List of Figures

1	Schematic diagram of a two-dimensional Ising spin lattice with nearest neighbour interactions J_x and J_y in an antiferromagnetic configuration. The dotted red line is a domain boundary that separates two opposite spin-oriented regions and is running in the x - or (10)-direction.	3
2	Illustration of a boundary segment and three kinks with lengths 1,2 and 3 in the (01)-direction. The green box indicates the spins we consider for the Hamiltonian.	5
3	Phase diagram of the two-dimensional square Ising model with anisotropic nearest neighbour interactions $ J_{x,y} /k_bT_c$ and external magnetic field influence h/k_bT_c . The grey planes indicate the conditions that $ J < h$	10
4	Cross sections of the phase diagram of figure 3 where $J_y = J_x$ (red line). The dashed lines indicate whenever $J_x = h $, the black lines indicate the ferromagnetic alignment condition $2 J < h$ as found in section 2.6.1.	11
5	Cross sections of the phase diagram of figure 3 where $J_y = 2J_x$. The black lines indicate the condition $2J_x = h $ as well as the ferromagnetic alignment condition $2 J < h$ as found in section 2.6.1.	12
6	Cross section of the phase diagram of figure 3 where $J_y = \frac{1}{2}J_x$. The dashed lines indicate whenever $\frac{1}{2}J_x = h $, the black lines indicate the ferromagnetic alignment condition $2 J < h$ as found in section 2.6.1.	12
7	Two of the many possible ground states for higher magnetic field strengths .	17
8	Phase diagram of the two-dimensional square Ising model with anisotropic nearest neighbour interactions $ J_{x,y} /k_bT_c$ and external magnetic field influence h/k_bT_c . The blue surface is the phase diagram including the $\ln(2)$ term as in equation 20. The red surface is the phase diagram as in figure 3. The grey planes indicate the conditions that $ J < h$	18
9	Cross sections of the blue phase diagram of figure 8 where $J_y = J_x$ (red line). The dashed lines indicate whenever $J_x = h $, the black lines indicate the ferromagnetic alignment condition $2 J < h$ as found in section 2.6.1.	19
10	Cross sections of the phase diagram of figure 3 where $J_y = \frac{1}{4}J_x$. The dashed lines indicate the condition $\frac{1}{4}J_x = h $ and the black lines depict the ferromagnetic alignment condition $2 J < h$ as found in section 2.6.1. We clearly see the phase boundary exceeding the non-negativity conditions for the formation energy.	20
11	Illustration of a boundary segment and three kinks with lengths 1,2 and 3 in the (01)-direction. The green box indicates the spins we consider for the Hamiltonian.	25
12	Phase diagram of the two-dimensional square Ising model with isotropic nearest neighbour interaction. The red line indicates the critical temperature T_c and the dashed lines indicate whenever $J = h$ or $J = -h$. The black lines indicate the ferromagnetic alignment condition $2 J < h$ as found in section 2.6.1.	30

The effect of an external magnetic field on an antiferromagnetic two-dimensional square Ising model with anisotropic nearest neighbour interaction

W.F.G. Rorink*

June 25, 2024

Abstract

An analytic expression for the phase boundary equation of the two-dimensional anti-ferromagnetic Ising square lattice with anisotropic nearest neighbour ($J_x \neq J_y$) interactions under the influence of a constant external magnetic field (h) is derived using the domain wall method. The system undergoes an order-disorder phase transition at a critical temperature $T = T_c$ that is given by the condition:

$$e^{(-2J_y+2h-4ph)/k_bT_c}(1 - e^{4J_x/k_bT_c}) = 1 + e^{4J_x/k_bT_c} + e^{(2J_x+2h)/k_bT_c} + e^{(2J_x-2h)/k_bT_c}.$$

The phase diagram for this condition is also derived. For vanishing magnetic field Onsager's famous result, i.e. $\sinh(2J_x/k_bT_c) \sinh(2J_y/k_bT_c) = 1$ is recaptured. We also show that the domain wall method is exact and we conjecture that the entire system can be described by a domain wall of minimal length.

Keywords: Ising model; domain wall free energy; external magnetic field; order-disorder phase transition; phase diagram

1 Introduction

Phase transitions are omnipresent within nature, familiar examples are the transition from liquid water to ice or the melting of iron in a foundry. Despite the abundance of phase transitions in the real world, the mathematical descriptions of these transitions are in many cases lacking. This is due to the complexity of the phase transitions since particles will often behave differently in the different phases. Furthermore, the phase transition can depend on many circumstances inside and outside the material. Within the field of statistical mechanics, a handful of phase transitions have been solved exactly as can be seen in [1], others are often approximated numerically.

One of the simplest models to describe order-disorder phase transitions is the so-called Ising model. In 1925 Ernst Ising considered a one-dimensional chain of spins which he used to describe ferromagnetism, see [2]. In this model, a spin, s , can point either upward, $s = +1$ or downward, $s = -1$. These spins are assumed to only interact with their nearest neighbour by a spin-spin coupling constant J . This coupling constant is an indication of how neighbouring spins prefer to align. If $J > 0$ the spins prefer a ferromagnetic configuration if $J < 0$ an antiferromagnetic configuration is preferred. Ising found that the one-dimensional spin chain was only ordered at $T = 0K$ and would be disordered at

*Email: w.f.g.rorink@student.utwente.nl

any other temperature. Based on this result Ising hypothesised that this would also be the case for the two- and three-dimensional case, but in 1936 Peiers showed that the two- and three-dimensional models have a nonzero phase transition temperature [3]. Below this critical temperature, T_c , the systems are in an ordered, i.e. (anti)ferromagnetic, state, whereas above this temperature the systems are in a disordered, i.e. paramagnetic, state.

Eventually, in 1944 Lars Onsager exactly solved the two-dimensional square Ising model in the absence of a magnetic field [4]. Here he found that this model indeed exhibits an order-disorder phase transition at a nonzero temperature. Onsager derived a closed and unique relation for the phase transition temperature which is given by

$$\sinh(2J_x/k_bT_c) \sinh(2J_y/k_bT_c) = 1 \quad (1)$$

After this publication of the exact solution of the square two-dimensional Ising model with nearest neighbour interaction in the absence of a magnetic field, the Ising model became a popular model for these phase transitions and was extended to also include a triangular lattice [5] or next-nearest neighbour interactions [6]. The Ising model and its more general version, the so-called Potts model, can be applied in a variety of other fields [7]. One example of this can be found within mathematics where several NP-optimisation problems can be described by an energy minimisation problem of a certain Ising model. The model has also been applied in the field of econophysics, where the volatility of returns can be modelled by a specific Ising model.

Despite the vast number of papers that have been published on the two-dimensional Ising model, many worked in the absence of an external magnetic field. This work aims to derive a closed expression of a square antiferromagnetic two-dimensional Ising model with anisotropic nearest neighbour interactions under the influence of an external homogeneous magnetic field. To derive this expression we will follow a method from literature where we will consider the free energy of the domain wall between two regions of opposite antiferromagnetic configuration as can be seen in [6, 8, 9]. At zero temperature the boundary is as straight as possible but with an increase in temperature more kinks will develop and the internal energy (U) of the system will increase, but also the entropy (S) of the system will increase. At a critical point, when the free energy ($F = U - TS$) of the boundary is zero, the system will undergo a phase transition from ordered to disordered.

2 Anisotropic Derivation

Consider a two-dimensional square lattice with anisotropic nearest neighbour interaction i.e. $J_x \neq J_y$ (A derivation for the isotropic case can be found in appendix A). The spin-spin interactions are assumed to be antiferromagnetic, i.e. $J < 0$. We also consider a constant magnetic field h in the spin-up direction, i.e. $h > 0$. The Hamiltonian of this system is then given by:

$$H = - \sum_{(i,j)} J_n s_i s_j - h \sum_i s_i \quad (2)$$

Here the first sum runs over all nearest neighbour spins and J_n can be either J_x or J_y .

2.1 Boundary formation

Let us now consider a boundary running in the x - or (10) -direction that separates two regions with opposite antiferromagnetic configurations, as shown in figure 1. The formation of such a boundary segment depends on the spin-spin interaction between the two regions and the orientation of the magnetic field. Because the formation energy depends on the magnetic field's presence, we need to consider the up-up and down-down interactions separately. This energy is found by determining the energy required to flip a certain spin configuration. For example, if we want to determine the formation energy for an up-up, or $\uparrow\uparrow$ boundary segment we see from the Hamiltonian (equation 2) that this costs an energy of $H_{\uparrow\uparrow} = -J_y - 2h$ to make if we want to change this from $\uparrow\downarrow$ or $\downarrow\uparrow$ this has an energy of $H_{\uparrow\downarrow} = J_y$ that needs to be overcome, so the formation energy per unit length is then $E_{Form,\uparrow\uparrow} = \Delta H = -2J_y - 2h$. The formation energy per unit length of the boundary segment is given by equation 3 for the up-up interactions and by equation 4 for the down-down interactions.

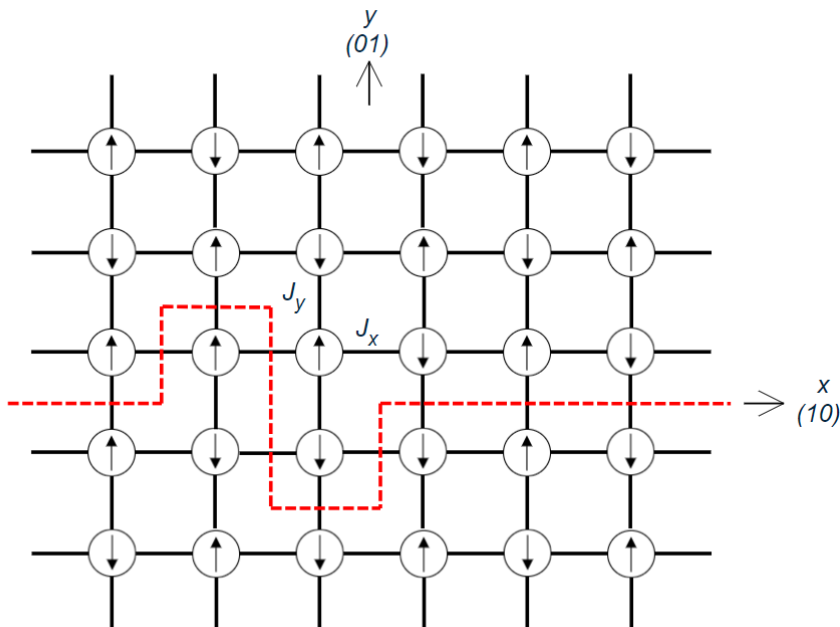


FIGURE 1: Schematic diagram of a two-dimensional Ising spin lattice with nearest neighbour interactions J_x and J_y in an antiferromagnetic configuration. The dotted red line is a domain boundary that separates two opposite spin-oriented regions and is running in the x - or (10) -direction.

$$E_{Form,\uparrow\uparrow} = -2J_y - 2h \quad (3)$$

$$E_{Form,\downarrow\downarrow} = -2J_y + 2h \quad (4)$$

For the boundary segment to physically form, this formation energy should be positive, i.e. $E_{Form} > 0$. We obtain the following conditions for J_y and h from equations 3 and 4:

- i) $J_y < h$
- ii) $-J_y > h$

Here the first condition is already met since $J_y < 0$ and $h > 0$ by assumption of the model. However, the second condition states that the spin-spin interaction J_y should be stronger than the magnetic field strength h . This makes physical sense, since for stronger magnetic fields than interactive forces the spins are forced in alignment with the magnetic field and a ferromagnetic configuration is formed [10]. When the magnetic field points in the opposite direction the roles of conditions i and ii would switch.

2.2 Kink formation

At zero temperature the boundary is as straight as possible, but with the increase in temperature, the boundary wall can form more kinks allowing the wall to meander through the lattice. This wandering increases the energy of the system but also increases the entropy of the system. This decreases the free energy of the domain wall since the free energy follows from $F = U - TS$. A kink's formation energy depends on the kink's length, n , in the y - or (01)-direction and the magnetic field strength, so we again need to consider the position of the kink. In figure 2 three kinks are depicted with length $n = 1, 2, 3$ which form *after* a step in the $\downarrow\downarrow$ -direction, here the formation energy in the (10)- and (01)-directions are both shown, these are calculated in the same way as before, this can also be done for a kink after a step in the $\uparrow\uparrow$ -direction. We observe a regularity in the formation energy per unit length of the boundary segment. This is given by equation 5 for a kink, after an up-up boundary segment, in the (01)-direction and by equation 6 for a kink, after a down-down boundary segment, in the (01)-direction.

$$E_{Kink,\uparrow\uparrow} = -2nJ_x - h(1 + (-1)^{n+1}) \text{ where } n \in \mathbb{N} \quad (5)$$

$$E_{Kink,\downarrow\downarrow} = -2nJ_x + h(1 + (-1)^{n+1}) \text{ where } n \in \mathbb{N} \quad (6)$$

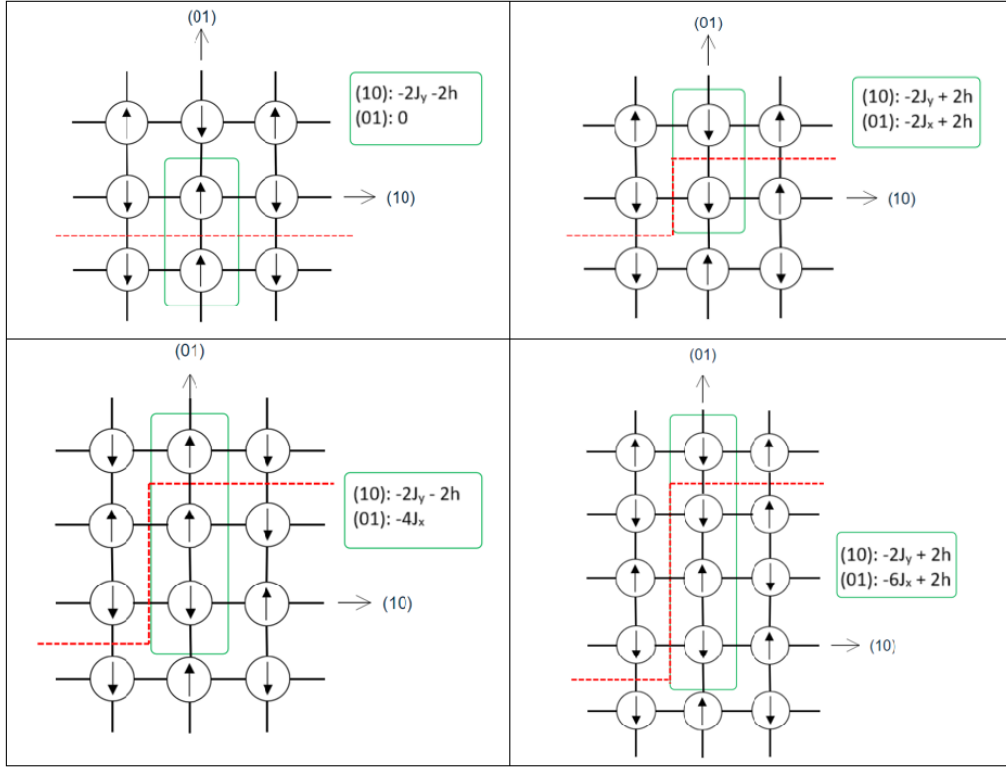


FIGURE 2: Illustration of a boundary segment and three kinks with lengths 1, 2 and 3 in the (01)-direction. The green box indicates the spins we consider for the Hamiltonian.

2.3 Partition function

With these formation energies for the boundary, we can set up the partition function for the boundary in the (10)-direction going through a $\uparrow\uparrow$ or $\downarrow\downarrow$ pair. We must consider all possible routes to make one step in the (10)-direction. This can be straight on or with a kink of length n in either (01)-direction. This gives the following partition functions:

$$Z_{\uparrow\uparrow} = e^{-(-2J_y - 2h)/k_b T} \left(1 + \frac{1}{2} \cdot 2 \sum_{n=1}^{\infty} e^{-(-2nJ_x + h(1 + (-1)^{n+1}))/k_b T} + \frac{1}{2} \cdot 2 \sum_{n=1}^{\infty} e^{-(-2nJ_x - h(1 + (-1)^{n+1}))/k_b T} \right) \quad (7)$$

and

$$Z_{\downarrow\downarrow} = e^{-(-2J_y + 2h)/k_b T} \left(1 + \frac{1}{2} \cdot 2 \sum_{n=1}^{\infty} e^{-(-2nJ_x + h(1 + (-1)^{n+1}))/k_b T} + \frac{1}{2} \cdot 2 \sum_{n=1}^{\infty} e^{-(-2nJ_x - h(1 + (-1)^{n+1}))/k_b T} \right). \quad (8)$$

The factor 2 in the partition function arises because the boundary can kink both upward and downward [6], as can be seen in figure 1. The factor 1/2 arises because the spin couples point up or down half of the lattice due to the antiferromagnetic ordering [10]. Equations 7 and 8 describe the different possibilities for the boundary to move through the different spin directions. Due to the magnetic field, one direction is energetically more favourable

than the other since the formation energy for the $\uparrow\uparrow$ step costs less energy than the $\downarrow\downarrow$ step. Therefore the partition function for the boundary in general will be:

$$Z_{(10)} = Z_{\uparrow\uparrow}^p Z_{\downarrow\downarrow}^{1-p}, \quad (9)$$

here p is the probability that the boundary moves through a $\uparrow\uparrow$ couple. Looking at equations 7 and 8 we see that

$$Z_{\uparrow\uparrow} = e^{4h/k_b T} \cdot Z_{\downarrow\downarrow}. \quad (10)$$

From this it follows that the probability p should be:

$$p = \frac{Z_{\uparrow\uparrow}}{Z_{\uparrow\uparrow} + Z_{\downarrow\downarrow}} = \frac{e^{4h/k_b T}}{e^{4h/k_b T} + 1} = \frac{1}{e^{-4h/k_b T} + 1}. \quad (11)$$

The total partition function of one step in the (10)-direction can then be described by:

$$Z_{(10)} = \left[e^{-(2J_y - 2h)/k_b T} \left(1 + \sum_{n=1}^{\infty} e^{-(-2nJ_x + h(1+(-1)^{n+1}))/k_b T} + \sum_{n=1}^{\infty} e^{-(-2nJ_x - h(1+(-1)^{n+1}))/k_b T} \right) \right]^p \cdot \left[e^{-(2J_y + 2h)/k_b T} \left(1 + \sum_{n=1}^{\infty} e^{-(-2nJ_x + h(1+(-1)^{n+1}))/k_b T} + \sum_{n=1}^{\infty} e^{-(-2nJ_x - h(1+(-1)^{n+1}))/k_b T} \right) \right]^{1-p}. \quad (12)$$

If want to consider the total partition function for a longer piece of boundary steps, say m steps, then it follows that

$$Z_{total} = Z_{(10)} \cdot Z_{(10)} \cdot \dots \cdot Z_{(10)} = Z_{(10)}^m. \quad (13)$$

For the free energy of a boundary segment of this length, we then find $F_{total} = -k_b T \ln(Z_{total}) = -mk_b T \ln(Z_{(10)})$. Whenever $F_{total} = 0$ we can divide the m out. So for our further derivation, we only need to consider one step.

2.4 Absolute convergence of the infinite series

Within the partition function of equation 12 we observe two infinite series concerning the kinks of the boundary. We want to rewrite these series in a closed form, therefore we would like these series to behave like geometric series. Before we can write down the series as a closed form we must be able to rewrite the series in the partition function in such a way that the oscillating term $h(1 + (-1)^{n+1})$ disappears and we can split each series into two geometric series. To achieve this, we want to make use of theorem 1 as found in [11].

Theorem 1 (Rearrangement Theorem for absolutely convergent series).

If the infinite series $\sum_{k=1}^{\infty} a_k$ is absolutely convergent then we can rearrange the terms of the series in such a way that the original series is equal to the sum of all the even and odd terms, i.e.

$$\sum_{k=1}^{\infty} a_k = \sum_{k=1}^{\infty} a_{2k} + \sum_{k=1}^{\infty} a_{2k-1}$$

This theorem needs that the series are absolutely convergent such that we can split the series into its odd and even terms. To show that the series are absolutely convergent we will prove the following lemma:

Lemma 1 (Absolute convergence of the series).

The series $\sum_{n=1}^{\infty} e^{-(-2nJ_x+h(1+(-1)^{n+1}))/k_bT}$ and $\sum_{n=1}^{\infty} e^{-(-2nJ_x-h(1+(-1)^{n+1}))/k_bT}$ are absolutely convergent under the conditions that $J_x < 0$ and $J_x < h$.

Proof. Consider the series $\sum_{n=1}^{\infty} e^{-(-2nJ_x \pm h(1+(-1)^{n+1}))/k_bT}$. For these series to be absolutely convergent it must hold that $\sum_{n=1}^{\infty} |e^{-(-2nJ_x \pm h(1+(-1)^{n+1}))/k_bT}| < \infty$.

Notice that

$$\sum_{n=1}^{\infty} |e^{-(-2nJ_x \pm h(1+(-1)^{n+1}))/k_bT}| = \sum_{n=1}^{\infty} e^{-(-2nJ_x \pm h(1+(-1)^{n+1}))/k_bT},$$

since $e^x > 0$ for all $x \in \mathbb{R}$.

To show this series is absolutely convergent we will apply the root test as found in [11] that is described by theorem 6 in appendix B. For our series, this becomes:

$$r = \limsup_{n \rightarrow \infty} |e^{-(-2nJ_x \pm h(1+(-1)^{n+1}))/k_bT}|^{1/n} = \limsup_{n \rightarrow \infty} e^{-(-2J_x \pm \frac{h}{n}(1+(-1)^{n+1}))/k_bT}.$$

We see that as n increases that the expressions $e^{-(-2J_x \pm \frac{h}{n}(1+(-1)^{n+1}))/k_bT}$ are bounded above, so we can write:

$$e^{-(-2J_x + \frac{h}{n}(1+(-1)^{n+1}))/k_bT} \leq e^{-(-2J_x)/k_bT}$$

and

$$e^{-(-2J_x - \frac{h}{n}(1+(-1)^{n+1}))/k_bT} \leq e^{-(-2J_x - 2h)/k_bT}.$$

So for our two series, we find:

$$r = e^{-(-2J_x)/k_bT}$$

and

$$r = e^{-(-2J_x - 2h)/k_b T}.$$

Because $J_x < 0$ and $J_x < h$ it follows that $r < 1$ in both cases, hence both series are absolutely convergent. \square

Both of the conditions used in the proof for the absolute convergence already hold by the assumptions of the model and the conditions for the formation energy, so they are also met at this point in our derivation. If the magnetic field would point in the opposite direction the same conditions would still hold due to the symmetry of the two series but each condition would apply to the other series.

Because we have proven that both series are absolutely convergent, we may now apply theorem 1 and we find the closed expressions:

$$\begin{aligned} \sum_{n=1}^{\infty} e^{-(-2nJ_x + h(1+(-1)^{n+1}))/k_b T} &= \sum_{n=1}^{\infty} e^{-(-4nJ_x)/k_b T} + \sum_{n=1}^{\infty} e^{-(-4nJ_x + 2J_x + 2h)/k_b T} \\ &= \frac{e^{4J_x/k_b T}}{1 - e^{4J_x/k_b T}} + \frac{e^{(2J_x - 2h)/k_b T}}{1 - e^{4J_x/k_b T}} = \frac{e^{4J_x/k_b T} + e^{(2J_x - 2h)/k_b T}}{1 - e^{4J_x/k_b T}} \end{aligned}$$

and

$$\begin{aligned} \sum_{n=1}^{\infty} e^{-(-2nJ_x - h(1+(-1)^{n+1}))/k_b T} &= \sum_{n=1}^{\infty} e^{-(-4nJ_x)/k_b T} + \sum_{n=1}^{\infty} e^{-(-4nJ_x + 2J_x - 2h)/k_b T} \\ &= \frac{e^{4J_x/k_b T}}{1 - e^{4J_x/k_b T}} + \frac{e^{(2J_x + 2h)/k_b T}}{1 - e^{4J_x/k_b T}} = \frac{e^{4J_x/k_b T} + e^{(2J_x + 2h)/k_b T}}{1 - e^{4J_x/k_b T}}. \end{aligned}$$

2.5 Phase Boundary Equation

With these results, we can rewrite the partition function of equation 12 as follows:

$$\begin{aligned} Z_{(10)} &= \left[e^{-(-2J_y - 2h)/k_b T} \left(1 + \frac{2e^{4J_x/k_b T} + e^{(2J_x + 2h)/k_b T} + e^{(2J_x - 2h)/k_b T}}{1 - e^{4J_x/k_b T}} \right) \right]^p \\ &\cdot \left[e^{-(-2J_y + 2h)/k_b T} \left(1 + \frac{2e^{4J_x/k_b T} + e^{(2J_x + 2h)/k_b T} + e^{(2J_x - 2h)/k_b T}}{1 - e^{4J_x/k_b T}} \right) \right]^{1-p}. \end{aligned} \quad (14)$$

With this closed form partition function, we are able to prove the following theorem:

Theorem 2 (Phase Boundary Equation).

The phase boundary equation of the antiferromagnetic two-dimensional square Ising model with anisotropic nearest neighbour interaction is given by:

$$e^{(-2J_y + 2h - 4ph)/k_b T_c} (1 - e^{4J_x/k_b T_c}) = 1 + e^{4J_x/k_b T_c} + e^{(2J_x + 2h)/k_b T_c} + e^{(2J_x - 2h)/k_b T_c}$$

Proof. With the partition function of equation 14 we can calculate the free energy of the system:

$$F_{(10)} = -k_b T \ln(Z_{(10)}) = -2J_y + 2h - 4ph - k_b T p \ln \left(1 + \frac{2e^{4J_x/k_b T} + e^{(2J_x+2h)/k_b T} + e^{(2J_x-2h)/k_b T}}{1 - e^{4J_x/k_b T}} \right) - k_b T (1-p) \ln \left(1 + \frac{2e^{4J_x/k_b T} + e^{(2J_x+2h)/k_b T} + e^{(2J_x-2h)/k_b T}}{1 - e^{4J_x/k_b T}} \right). \quad (15)$$

The critical temperature can be found by setting the domain wall free energy to zero, i.e. $F_{(10)} = 0$. This gives the expression:

$$-2J_y + 2h - 4ph = k_b T_c p \ln \left(1 + \frac{2e^{4J_x/k_b T_c} + e^{(2J_x+2h)/k_b T_c} + e^{(2J_x-2h)/k_b T_c}}{1 - e^{4J_x/k_b T_c}} \right) + k_b T_c (1-p) \ln \left(1 + \frac{2e^{4J_x/k_b T_c} + e^{(2J_x+2h)/k_b T_c} + e^{(2J_x-2h)/k_b T_c}}{1 - e^{4J_x/k_b T_c}} \right). \quad (16)$$

Since the right-hand side is of the form $p \cdot A + (1-p) \cdot A$, we can simplify this to:

$$-2J_y + 2h - 4ph = k_b T_c \ln \left(1 + \frac{2e^{4J_x/k_b T_c} + e^{(2J_x+2h)/k_b T_c} + e^{(2J_x-2h)/k_b T_c}}{1 - e^{4J_x/k_b T_c}} \right). \quad (17)$$

This gives the following phase boundary equation:

$$e^{(-2J_y+2h-4ph)/k_b T_c} (1 - e^{4J_x/k_b T_c}) = 1 + e^{4J_x/k_b T_c} + e^{(2J_x+2h)/k_b T_c} + e^{(2J_x-2h)/k_b T_c}, \quad (18)$$

where p is still defined as in equation 11. \square

2.6 Phase diagrams

With the phase boundary equation of equation 18 we can develop the phase diagram of the system, this can be seen in figure 3. This figure also includes the conditions that the coupling constants J_x and J_y should be greater than the magnetic field strength h , this is indicated by the grey planes. In this figure, the magnetic field can point in either the up, $h > 0$, or down $h < 0$ direction, since the same result will be acquired when the direction of h flips.

Figure 3 shows that for low $J_x/k_b T_c$ compared to $J_y/k_b T_c$ or vice versa we see that the condition that $J < h$ is not met, this can be explained by the fact that in this case the antiferromagnetic configuration almost decouples into one-dimensional chains which violates the assumptions of the model. This effect is stronger for J_y compared to J_x since the magnetic field influences the formation energy of a boundary step more directly than a boundary kink.

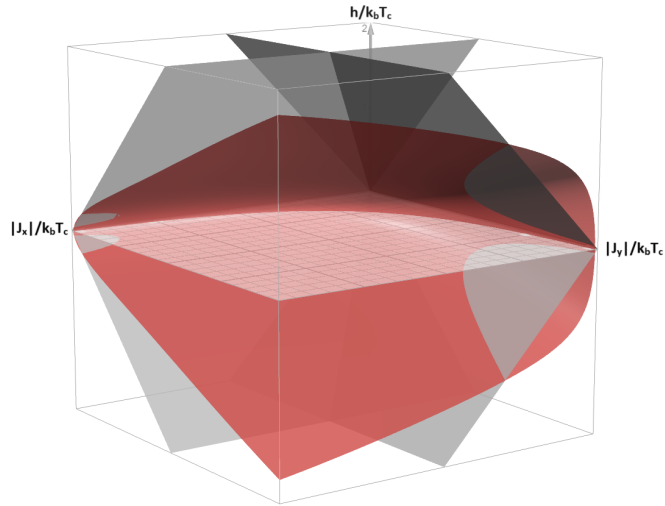


FIGURE 3: Phase diagram of the two-dimensional square Ising model with anisotropic nearest neighbour interactions $|J_{x,y}|/k_b T_c$ and external magnetic field influence $h/k_b T_c$. The grey planes indicate the conditions that $|J| < h$.

2.6.1 Ferromagnetic alignment condition

If we look at the Hamiltonian in equation 2 we can determine an approximation for when the system will align ferromagnetically due to the magnetic field even though $J < 0$. For an antiferromagnetic configuration in an isotropic case, we find an energy of $2J + h$, while a ferromagnetic configuration gives an energy of $-2J - h$. So we find that the system is forced in a ferromagnetic configuration whenever:

$$-2J - h < 2J + h.$$

Or more simply:

$$2|J| < h.$$

This relation is not exact and will act more as a condition for when the system is forced from a disordered paramagnetic phase to an ordered ferromagnetic phase due to the magnetic field.

2.6.2 Isotropic phase diagram

Figure 4 shows the phase diagram for the isotropic case, i.e. $J_x = J_y$. This diagram is identical to the phase diagram found in the isotropic derivation in appendix A.

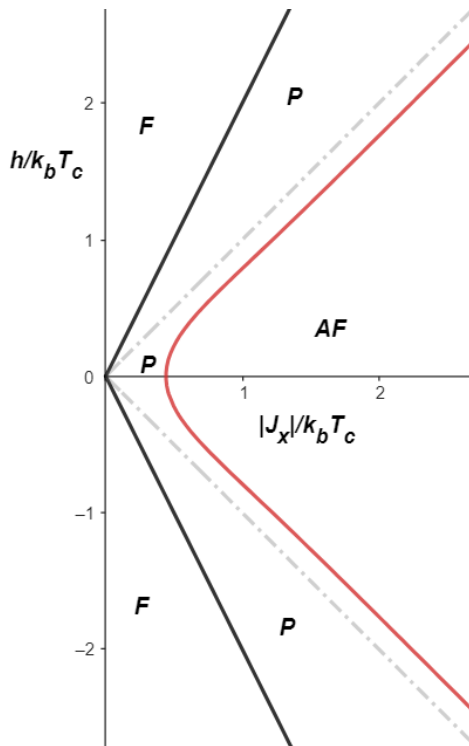


FIGURE 4: Cross sections of the phase diagram of figure 3 where $J_y = J_x$ (red line). The dashed lines indicate whenever $J_x = |h|$, the black lines indicate the ferromagnetic alignment condition $2|J| < h$ as found in section 2.6.1.

In this figure, we see a clear antiferromagnetic (AF) region whenever the spin-spin interaction J_x is strong enough and J_x is stronger than the magnetic field h . In the vicinity of the Onsager point, i.e. $\frac{J_x}{k_b T_c} = \frac{1}{2} \ln(\sqrt{2} + 1) \approx 0.4406867\dots$ and $h = 0$, we see that for $J < |h|$ a paramagnetic (P) region occurs. Here the spin-spin interaction is not strong enough to form an antiferromagnetic configuration and the magnetic field is not strong enough to align all the spins into a ferromagnetic (F) configuration. This transition indicates an order-disorder phase transition. Around the condition that $J_x = |h|$ we see that the system is already in the paramagnetic phase, this implies that the system will transition to the disordered state before the magnetic field is as strong as the spin-spin interaction. This could be attributed to the effect of the degeneracy of the different ground states of the model, more on that in section 3.1.

2.6.3 Anisotropic phase diagrams

In figure 5 we see the phase diagram for the anisotropic case that $J_y = 2J_x$. This diagram, like the isotropic case, shows that the system will go into a paramagnetic phase before $J_x = |h|$. In figure 6 the anisotropic case that $J_y = \frac{1}{2}J_x$ is shown. Here we see that the phase boundary equation will very soon obey the condition that $J = |h|$, this is the boundary case before the system exceeds the conditions as shown in the full phase diagram in figure 3.

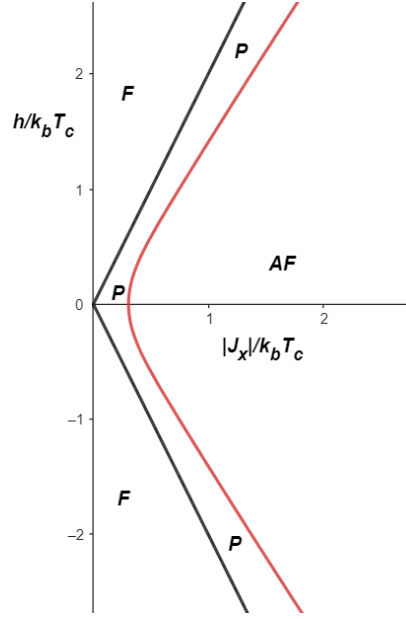


FIGURE 5: Cross sections of the phase diagram of figure 3 where $J_y = 2J_x$. The black lines indicate the condition $2J_x = |h|$ as well as the ferromagnetic alignment condition $2|J| < h$ as found in section 2.6.1.

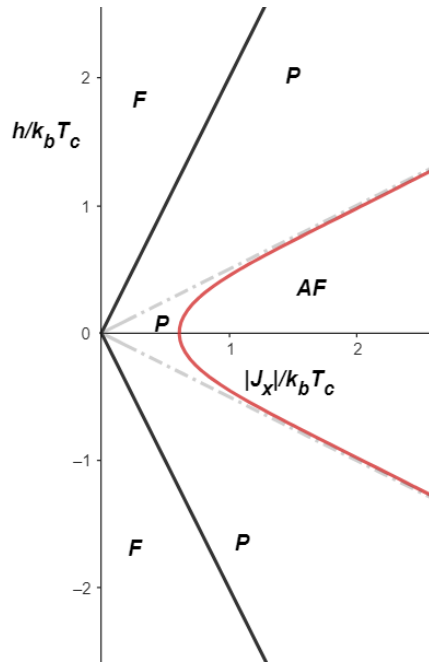


FIGURE 6: Cross section of the phase diagram of figure 3 where $J_y = \frac{1}{2}J_x$. The dashed lines indicate whenever $\frac{1}{2}J_x = |h|$, the black lines indicate the ferromagnetic alignment condition $2|J| < h$ as found in section 2.6.1.

2.7 Vanishing magnetic field

When we consider a vanishing magnetic field in expression 16, i.e. $h \rightarrow 0$ we find:

$$2J_y = -k_b T_c \ln \left(1 + \frac{2e^{4J_x/k_b T_c} + 2e^{2J_x/k_b T_c}}{1 - e^{4J_x/k_b T_c}} \right)$$

Note that

$$\frac{2e^{2x} + 2e^{4x}}{1 - e^{4x}} = \frac{2e^{2x}(1 + e^{2x})}{(1 - e^{2x})(1 + e^{2x})} = \frac{2e^{2x}}{1 - e^{2x}} \text{ for } x \neq 0$$

Since $x = J_x/k_b T_c \neq 0$, we find:

$$2J_y = -k_b T_c \ln \left(1 + \frac{2e^{2J_x/k_b T_c}}{1 - e^{2J_x/k_b T_c}} \right) \quad (19)$$

This is equivalent to Onsager's expression for the Ising model without an external magnetic field with anisotropic nearest neighbour interaction as can be found in [4]. The derivation from equation 19 to the famous result of Onsager in equation 1 can be proven by the following lemma:

Lemma 2 (Equivalence to Onsager's result).

$2J_y = -k_b T_c \ln \left(1 + \frac{2e^{2J_x/k_b T_c}}{1 - e^{2J_x/k_b T_c}} \right)$ is equivalent to $\sinh \left(\frac{2J_x}{k_b T_c} \right) \sinh \left(\frac{2J_y}{k_b T_c} \right) = 1$ under the conditions that $J_x \neq 0$ and $J_y \neq 0$

Before we can start the proof, we will need some definitions and identities of hyperbolic functions:

Necessary hyperbolic relations

1. $\sinh(x) = \frac{e^x - e^{-x}}{2}$
 2. $\cosh^2(x) - \sinh^2(x) = 1$
 3. $\tanh(x) = \frac{\sinh(x)}{\cosh(x)} = \frac{e^{2x} - 1}{e^{2x} + 1}$
 4. $\tanh\left(\frac{x}{2}\right) = \frac{\cosh(x) - 1}{\sinh(x)}$
-

Proof. We start with equation 19:

$$2J_y = -k_b T_c \ln \left(1 + \frac{2e^{2J_x/k_b T_c}}{1 - e^{2J_x/k_b T_c}} \right).$$

For the ferromagnetic case that Onsager considered we need to change J_x and J_y with $-J_x$ and $-J_y$, this gives:

$$2J_y = k_b T_c \ln \left(1 + \frac{2e^{-2J_x/k_b T_c}}{1 - e^{-2J_x/k_b T_c}} \right).$$

This can be rewritten into the following form:

$$e^{2J_y/k_b T_c} = 1 + \frac{2e^{-2J_x/k_b T_c}}{1 - e^{-2J_x/k_b T_c}}.$$

For simplicity we introduce: $x = J_x/k_b T_c$ and $y = J_y/k_b T_c$ this results in:

$$e^{2y} = 1 + \frac{2e^{-2x}}{1 - e^{-2x}}.$$

When we rewrite the right-hand side as one fraction we see:

$$e^{2y} = \frac{1 - e^{-2x} + 2e^{-2x}}{1 - e^{-2x}} = \frac{1 + e^{-2x}}{1 - e^{-2x}}.$$

Now we introduce the hyperbolic tangent by using relation 3:

$$e^{2y} = \frac{1}{\tanh(x)}.$$

Note that:

$$e^{-2y} = \tanh(x).$$

Next, we rewrite e^{2y} as a hyperbolic sine following the definition, this yields:

$$2 \sinh(2y) + e^{-2y} = \frac{1}{\tanh(x)}.$$

We replace e^{-2y} as follows:

$$2 \sinh(2y) + \tanh(x) = \frac{1}{\tanh(x)}.$$

This equation can be rewritten using relation 4, which gives the following:

$$2 \sinh(2y) = \frac{\sinh(2x)}{\cosh(2x) - 1} - \frac{\cosh(2x) - 1}{\sinh(2x)}.$$

This can be combined into one fraction:

$$2 \sinh(2y) = \frac{\sinh^2(2x) - (\cosh(2x) - 1)^2}{\sinh(2x) \cosh(2x) - \sinh(2x)}.$$

Expanding gives the following:

$$2 \sinh(2y) = \frac{\sinh^2(2x) - \cosh^2(2x) + 2 \cosh(2x) - 1}{\sinh(2x) \cosh(2x) - \sinh(2x)}.$$

We can now apply relation 2, this yields:

$$2 \sinh(2y) = \frac{2 \cosh(2x) - 2}{\sinh(2x) \cosh(2x) - \sinh(2x)}.$$

With some rewriting, we find:

$$\sinh(2y) = \frac{\cosh(2x) - 1}{\sinh(2x)(\cosh(2x) - 1)}.$$

This can be reduced to:

$$\sinh(2y) = \frac{1}{\sinh(2x)} \text{ since } x \neq 0.$$

Because $x \neq 0$ we can rewrite this expression to a more familiar equation:

$$\sinh\left(\frac{2J_x}{k_b T_c}\right) \sinh\left(\frac{2J_y}{k_b T_c}\right) = 1.$$

This is identical to Onsager's result in equation 1. Because $\sinh(x)$ is an odd function, i.e. $\sinh(-x) = -\sinh(x)$, it does not matter if we consider the antiferromagnetic or the ferromagnetic case, since both will yield the same result. \square

2.8 General Results

The previous section showed that the result for a vanishing magnetic field is equivalent to Onsager's result, this means that our result is in this case exact for all temperatures T . We did, however, ignore the cases where the boundary could form overhangs (i.e. moving back in the negative x -direction after a step in the y -direction) or inclusions (i.e. a loop of opposite spin within a region). Overhangs and loops add roughness to the domain wall and will thus increase the system's energy, so these are energetically unfavourable. With an increase in temperature, they could occur. In larger systems, however, their contributions seem to become irrelevant [12, 13]. This leads us to believe that in large systems the partition function using Onsager's method of describing the system is equivalent to the partition function found by the domain wall method. Since the free energies are equivalent we can say that the free energy found by the method employed by Onsager equals the free energy found by the domain wall method, i.e. $F_{\text{Onsager}} = F_{\text{DomainWall}}(h = 0)$. It follows then that $Z_{\text{Onsager}} = Z_{\text{DomainWall}}(h = 0)$. Thus, to prove this equivalence in partition functions we will prove the following theorem:

Theorem 3 (Equivalence of partition function).

The partition function that describes the entire system using Onsager's method, i.e. $Z_{\text{Onsager}} = e^{-E_1/k_b T} + e^{-E_2/k_b T} + \dots + e^{-E_n/k_b T}$ is equivalent for describing large systems to the partition function that describes the domain wall using our method without a magnetic field, i.e. $Z_{\text{DomainWall}}(h = 0) = e^{-E'_1/k_b T} + e^{-E'_2/k_b T} + \dots + e^{-E'_m/k_b T}$ for all T .

To prove this theorem we first need to state the following helpful theorem, found in [14]:

Theorem 4 (Equality of Power Sums).

Let a_i and b_j be two finite sequences of non-negative real numbers. If for all $x \in \mathbb{R}$, we have

$$\sum_i a_i^x = \sum_j b_j^x.$$

Then there exists a permutation σ of the indices such that

$$a_i = b_{\sigma(i)} \text{ for all } i.$$

Proof. Since $Z_{\text{Onsager}} = Z_{\text{DomainWall}}(h = 0)$ we find

$$e^{-E_1/k_b T} + e^{-E_2/k_b T} + \dots + e^{-E_n/k_b T} = e^{-E'_1/k_b T} + e^{-E'_2/k_b T} + \dots + e^{-E'_m/k_b T} \text{ for all } T.$$

Or more simply:

$$\sum_i^n e^{-E_i/k_b T} = \sum_j^m e^{-E'_j/k_b T} \text{ for all } T.$$

Set $x = 1/k_b T$ then:

$$\sum_i^n e^{-E_i x} = \sum_j^m e^{-E'_j x} \text{ for all } x.$$

This is equivalent to:

$$\sum_i^n (e^{-E_i})^x = \sum_j^m (e^{-E'_j})^x \text{ for all } x.$$

With this relation, we conclude that $n = m$ because otherwise, the sums would not be equal for all x since some e^x terms would dominate one side for large x if they are not compensated on the other side. Then we can apply theorem 4 since we have two finite non-negative real sequences whose sums are equal. This results in the fact that there exists a permutation σ of the indices such that:

$$e^{-E_i} = e^{-E'_{\sigma(i)}} \text{ for all } i.$$

From this, it follows that:

$$E_i = E'_{\sigma(i)} \text{ for all } i.$$

Hence we can conclude that each energy term in the partition function of Onsager's method has a corresponding term in the partition function of the domain wall method. This implies that the two partition functions are equivalent in describing the system. \square

Now that we have proven theorem 3 we can conclude that in larger systems the partition function using Onsager's method of describing the system is equivalent to the partition function found by the domain wall method. Since inclusions and overhangs seem to be irrelevant or perfectly cancel for large systems it looks like any domain wall can be reduced to the domain wall with minimal length in the direction of the domain wall. We denote this with the following conjecture:

Conjecture 1 (Minimal length).

For large enough systems, the partition function of the entire system can be described by the domain wall with minimum length in the direction of the domain wall.

This conjecture implies that we can describe large systems with the derivation used in this article, therefore it should follow that the entire system can be described with the same results. The magnetic field introduces an extra energy term. This influence could result in the fact that overhangs and inclusions become important to include, but for a small enough magnetic field these boundary shapes should remain negligible. We denote this with the following conjecture:

Conjecture 2 (Phase boundary equation).

If conjecture 1 is true, then for a small enough external magnetic field h the phase boundary given by the equation:

$$e^{(-2J_y+2h-4ph)/k_bT_c}(1 - e^{4J_x/k_bT_c}) = 1 + e^{4J_x/k_bT_c} + e^{(2J_x+2h)/k_bT_c} + e^{(2J_x-2h)/k_bT_c},$$

that is found using the domain wall method exactly describes the phase boundary of the entire system.

3 Discussion and conclusion

In this section, we will look at different factors that could influence our derivation and found results. We will look at different ground states of the system, the decoupling of the phase diagram in figure 3 and the correctness of the partition function. We will then conclude our work and give an outlook on further research using a similar derivation as used in this article.

3.1 Ground state of the boundary

The domain wall boundary will be as straight as possible in the ground state for a small magnetic field. However, with an increase in the magnetic field strength, it becomes more energetically favourable for the boundary to meander through the lattice and go through the spins that align with the magnetic field [15]. For two examples of this meandering see figure 7. This can also be seen from the formation of the boundary segments in equations 3 and 4 and the costs for the kinks in equations 5 and 6, where for high enough values of h it could be energetically more favourable to form a kink through the $\uparrow\uparrow$ spin couples than to go through the $\downarrow\downarrow$ pair without a kink. These boundaries are however vastly degenerate since there are 2^N different configurations for a lattice with domain wall length N which all have the same energy.

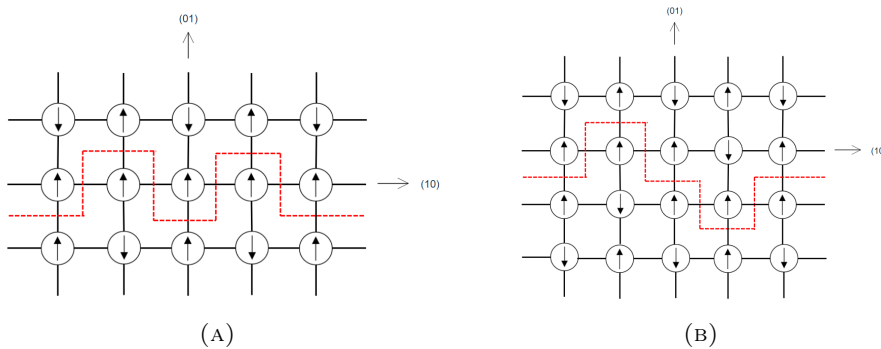


FIGURE 7: Two of the many possible ground states for higher magnetic field strengths

This degeneracy could explain the space between the phase boundary and the energy formation condition in figure 4, 5 and 6 since this degeneracy increases the entropy of the system and thus decrease the free energy of the system. It could also be that this degeneracy would introduce a factor of 2 in front of the partition function in equation 14 and thus a factor of $\ln(2)$ in the phase boundary equation of equation 18, this would then become:

$$e^{(-2J_y+2h-4ph)/k_bT_c}(1-e^{4J_x/k_bT_c}) = \ln(2)(1+e^{4J_x/k_bT_c}+e^{(2J_x+2h)/k_bT_c}+e^{(2J_x-2h)/k_bT_c}). \quad (20)$$

This would result in a slightly different phase diagram which looks like the blue surface in figure 8.

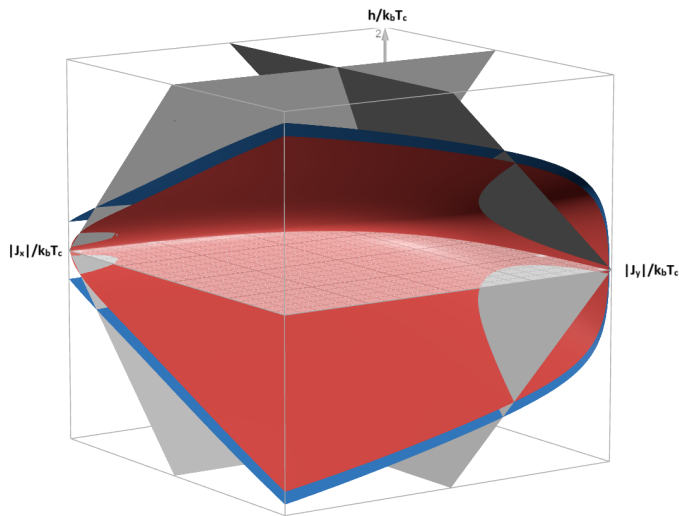


FIGURE 8: Phase diagram of the two-dimensional square Ising model with anisotropic nearest neighbour interactions $|J_{x,y}|/k_bT_c$ and external magnetic field influence h/k_bT_c . The blue surface is the phase diagram including the $\ln(2)$ term as in equation 20. The red surface is the phase diagram as in figure 3. The grey planes indicate the conditions that $|J| < h$.

For the isotropic case the phase diagram will look like figure 9.

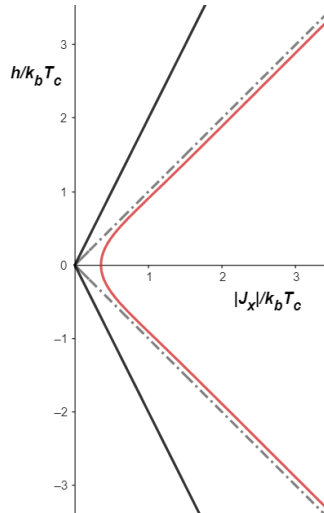


FIGURE 9: Cross sections of the blue phase diagram of figure 8 where $J_y = J_x$ (red line). The dashed lines indicate whenever $J_x = |h|$, the black lines indicate the ferromagnetic alignment condition $2|J| < h$ as found in section 2.6.1.

This extra $\ln(2)$ term would move the phase boundary closer to the condition for non-negative formation energy in the isotropic case. In general, this would mean that the system would decouple faster compared to our earlier found result with the phase boundary equation in equation 18. This factor would also result in a difference from Onsager's result due to the degeneracy of the ground state. Without the magnetic field, the model would only have one ground state with minimal energy, but since the magnetic field can 'help' the system find many ground states with lower energies by forming the domain boundary between the energetically favourable spin couples.

3.2 Decoupling in the phase diagrams

In figure 3 we see that whenever one spin-spin interaction is much larger than the other, this comes from the fact that for highly anisotropic behaviour the model effectively decouples into a series of one-dimensional Ising chains [16]. Since the interactions in one direction will dominate the coupling in the other direction becomes negligible. This results in the fact that the system will behave differently under these circumstances and will thus not be accurately described with the current two-dimensional approach since conditions like $J > |h|$ are not satisfied. This would lead to the formation energies for the boundaries and kinks to become negative, something which is not physically possible.

This phenomenon can be seen more clearly in figure 10. Here we see the phase boundary exceeding the condition that ensures the non-negativity of the domain boundary.

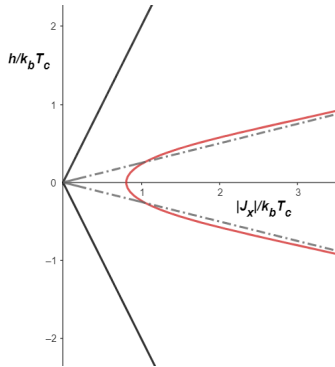


FIGURE 10: Cross sections of the phase diagram of figure 3 where $J_y = \frac{1}{4}J_x$. The dashed lines indicate the condition $\frac{1}{4}J_x = |h|$ and the black lines depict the ferromagnetic alignment condition $2|J| < h$ as found in section 2.6.1. We clearly see the phase boundary exceeding the non-negativity conditions for the formation energy.

3.3 Correctness of the partition function

With the domain wall method, we can easily reduce the dimension of the system by considering the domain boundary between two regions of opposite antiferromagnetic configuration. We have proven this method to be exact, but this method has its difficulties. One of the major difficulties is finding the correct partition function to describe all possible configurations of the domain boundary. Since this method stands or falls with the correctness of the partition function it is essential to determine the full contribution of each energy term. In our derivation multiple partition functions have been considered which would all recapture Onsager's result for a vanishing magnetic field, but would all give different limitations for describing the entire system. One partition function would not incorporate the probability of certain kinks being made more often instead of others due to the contribution of the magnetic field. Another would incorporate extra contributions of the magnetic field which were invalid. All in all the partition function of equation 12 and thus equation 14 seems to be the most accurate partition function to date. However, it may be possible that the factor $\frac{1}{2}$ in equation 12 should be replaced by a probability q of a certain kink occurring more often than the other to describe the system more carefully. Furthermore, it could also be possible that the factor 2 should be replaced by a probability r since the magnetic field could influence the boundary to prefer one direction of kinks compared to another.

3.4 Conclusion

We have derived a closed analytic expression for the phase boundary equation for the two-dimensional antiferromagnetic square Ising model with anisotropic nearest neighbour interactions by employing the domain wall method which relies on determining the domain wall free energy between two regions of opposite antiferromagnetic configuration. We have presented the three-dimensional phase diagram together with some two-dimensional phase diagrams for the isotropic case and two anisotropic cases. We found the order-disorder temperature relation. We also proved that the domain wall method exactly describes the entire system. Furthermore, we conjectured that the entire system can be described by the domain wall with minimum length in the direction of the boundary and the the phase boundary can be exactly determined using the domain wall method.

3.5 Outlook

In this derivation, we only looked at the effect of the external magnetic field on the antiferromagnetic two-dimensional square Ising model with anisotropic nearest neighbour interactions. This is only one small part of the entire study of phase transitions due to an external magnetic field. One could extend the same derivation as in this article to find the phase boundary equation for a hexagonal lattice. Within condensed-matter physics, many materials are structured in other arrangements than square, so looking into the behaviour of these phase transitions could provide more insight into our understanding of these phase transitions.

Moreover, we only estimated the condition for the forced ferromagnetic configuration due to the external magnetic field, it could be interesting to look at the exact relation for forcing the antiferromagnetic lattice into the ferromagnetic configuration. This would make the phase diagrams more complete and robust, which gives a better view of the behaviour of the system due to the external magnetic field.

In our analysis, we looked solely at the nearest-neighbour interaction. Extending the model with the influence of the next-nearest neighbours could provide more insight into the phase transition from antiferromagnetic to paramagnetic or ferromagnetic. The Hamiltonian of such a system looks like:

$$H = -J_x \sum_i s_{i,j} s_{i+1,j} - J_y \sum_j s_{i,j} s_{i,j+1} - J_d \sum_{(i,j)} (s_{i,j} s_{i+1,j+1} + s_{i,j} s_{i+1,j-1}) - h \sum_i s_i. \quad (21)$$

This analysis will however no longer be exact due to the next-nearest neighbour interaction since there will be a difference in energy contribution between a kinked and non-kinked boundary segment [9]. Nevertheless, this approximation could help with the understanding of the complexity of these phase transitions.

4 References

- ¹G. D’Ariano, A. Montorsi, M. Rasetti, and R. J. Baxter, “Exactly Solved Models in Statistical Mechanics”, en, in , Vol. 1, Book Title: Integrable Systems in Statistical Mechanics Series Title: Series on Advances in Statistical Mechanics (May 1985), pp. 5–63, ISBN: 978-9971-978-11-2 978-981-4415-25-5, 10.1142/9789814415255_0002.
- ²E. Ising, “Beitrag zur Theorie des Ferromagnetismus”, de, Zeitschrift für Physik **31**, 253–258, ISSN: 0044-3328 (1925) 10.1007/BF02980577.
- ³R. Peierls, “On Ising’s model of ferromagnetism”, en, Mathematical Proceedings of the Cambridge Philosophical Society **32**, 477–481, ISSN: 1469-8064, 0305-0041 (1936) 10.1017/S0305004100019174.
- ⁴L. Onsager, “Crystal Statistics. I. A Two-Dimensional Model with an Order-Disorder Transition”, Physical Review **65**, Publisher: American Physical Society, 117–149 (1944) 10.1103/PhysRev.65.117.
- ⁵L. Zhi-Huan, L. Mushtaq, L. Yan, and L. Jian-Rong, “Critical behaviour of the ferromagnetic Ising model on a triangular lattice”, en, Chinese Physics B **18**, 2696, ISSN: 1674-1056 (2009) 10.1088/1674-1056/18/7/012.
- ⁶H. J. W. Zandvliet, “The 2D Ising square lattice with nearest- and next-nearest-neighbor interactions”, en, Europhysics Letters **73**, Publisher: IOP Publishing, 747, ISSN: 0295-5075 (2006) 10.1209/epl/i2005-10451-1.
- ⁷A. Lipowski, “Ising Model: Recent Developments and Exotic Applications”, Entropy **24**, 1834, ISSN: 1099-4300 (2022) 10.3390/e24121834.
- ⁸H. Zandvliet and C. Hoede†, “Spontaneous magnetization of the square 2D Ising lattice with nearest- and weak next-nearest-neighbour interactions”, Phase Transitions **82**, Publisher: Taylor & Francis _eprint: <https://doi.org/10.1080/01411590802610163>, 191–196, ISSN: 0141-1594 (2009) 10.1080/01411590802610163.
- ⁹H. J. W. Zandvliet, “Phase diagram of the square 2D Ising lattice with nearest neighbor and next-nearest neighbor interactions”, Phase Transitions **96**, Publisher: Taylor & Francis _eprint: <https://doi.org/10.1080/01411594.2022.2162897>, 187–195, ISSN: 0141-1594 (2023) 10.1080/01411594.2022.2162897.
- ¹⁰E. M. Levin, “Antiferromagnet-ferromagnet transitions in ge-rich gd5 (six ge4-x) alloys induced by composition, magnetic field, and temperature”, Phys. Rev. B **80**, 144401 (2009) 10.1103/PhysRevB.80.144401.
- ¹¹W. R. Wade, *Introduction to analysis: pearson new international edition* (Pearson, Harlow, 2014), pp. 198–214, ISBN: 9781292039329.
- ¹²J. T. Clemmer and M. O. Robbins, “Anisotropic avalanches and critical depinning of three-dimensional magnetic domain walls”, Physical Review E **100**, Publisher: American Physical Society, 042121 (2019) 10.1103/PhysRevE.100.042121.
- ¹³N. J. Zhou and B. Zheng, “Dynamic effect of overhangs and islands at the depinning transition in two-dimensional magnets”, Physical Review E **82**, Publisher: American Physical Society, 031139 (2010) 10.1103/PhysRevE.82.031139.
- ¹⁴A. Caminha Muniz Neto, *An Excursion through Elementary Mathematics, Volume III*, Problem Books in Mathematics (Springer International Publishing, Cham, 2018), ISBN: 978-3-319-77976-8 978-3-319-77977-5, 10.1007/978-3-319-77977-5.

- ¹⁵E. Müller-Hartmann and J. Zittartz, “Interface free energy and transition temperature of the square-lattice Ising antiferromagnet at finite magnetic field”, en, *Zeitschrift für Physik B Condensed Matter* **27**, 261–266, ISSN: 1431-584X (1977) 10.1007/BF01325537.
- ¹⁶F. Etori, T. Coupé, T. J. Sluckin, E. Puppini, and P. Biscari, “Dynamic Phase Transition in 2D Ising Systems: Effect of Anisotropy and Defects”, en, *Entropy* **26**, Number: 2 Publisher: Multidisciplinary Digital Publishing Institute, 120, ISSN: 1099-4300 (2024) 10.3390/e26020120.

A Isotropic Derivation

Consider a two-dimensional square lattice with isotropic nearest neighbour interaction i.e. $J = J_x = J_y$. The spin-spin interactions are assumed to be antiferromagnetic, i.e. $J < 0$. We also consider a constant magnetic field h in the spin-up direction, i.e. $h > 0$. The Hamiltonian of this system is then given by

$$H = -J \sum_{(i,j)} s_i s_j - h \sum_i s_i \quad (22)$$

Here the first sum runs over all nearest neighbour spins.

A.1 Boundary and kink formation

Let us now consider a boundary running in the x - or (10) -direction that separates two regions with opposite antiferromagnetic configurations, as shown in figure 1. The formation of such a boundary segment depends on the spin-spin interaction between the two regions and the orientation of the magnetic field. Because the formation energy depends on the magnetic field's presence, we need to consider the up-up and down-down interactions separately. This energy is found by determining the energy required to flip a certain spin configuration. For example, if we want to determine the formation energy for an up-up, or $\uparrow\uparrow$ boundary segment we see from the Hamiltonian (equation 22) that this has an energy of $H_{\uparrow\uparrow} = -J - 2h$ if we want to change this from $\uparrow\downarrow$ or $\downarrow\uparrow$ this has energy $H_{\uparrow\downarrow} = J$, so the formation energy per unit length is then $E_{form,\uparrow\uparrow} = \Delta H = -2J - 2h$. The formation energy per unit length of the boundary segment is given by equation 23 for the up-up interactions and by equation 24 for the down-down interactions.

$$E_{form,\uparrow\uparrow} = -2J - 2h \quad (23)$$

$$E_{form,\downarrow\downarrow} = -2J + 2h \quad (24)$$

For the boundary segment to physically form, the formation energy should be positive, i.e. $E_{form} > 0$. We obtain the following conditions for J and h from equations 23 and 24:

- i) $J < h$
- ii) $-J > h$

Here the first condition is already met since $J < 0$ and $h > 0$ by assumption of the model. However, the second condition states that the spin-spin interaction J should be stronger than the magnetic field strength h . This makes physical sense, since for stronger magnetic fields than interactive forces the spins are forced in alignment with the magnetic field and a ferromagnetic configuration is formed [10]. When the magnetic field points in the opposite direction the roles of conditions i and ii would switch.

At zero temperature the boundary is as straight as possible, but with the increase in temperature, the boundary wall can form more kinks allowing the wall to meander through the lattice. This wandering increases the energy of the system but also increases the entropy of

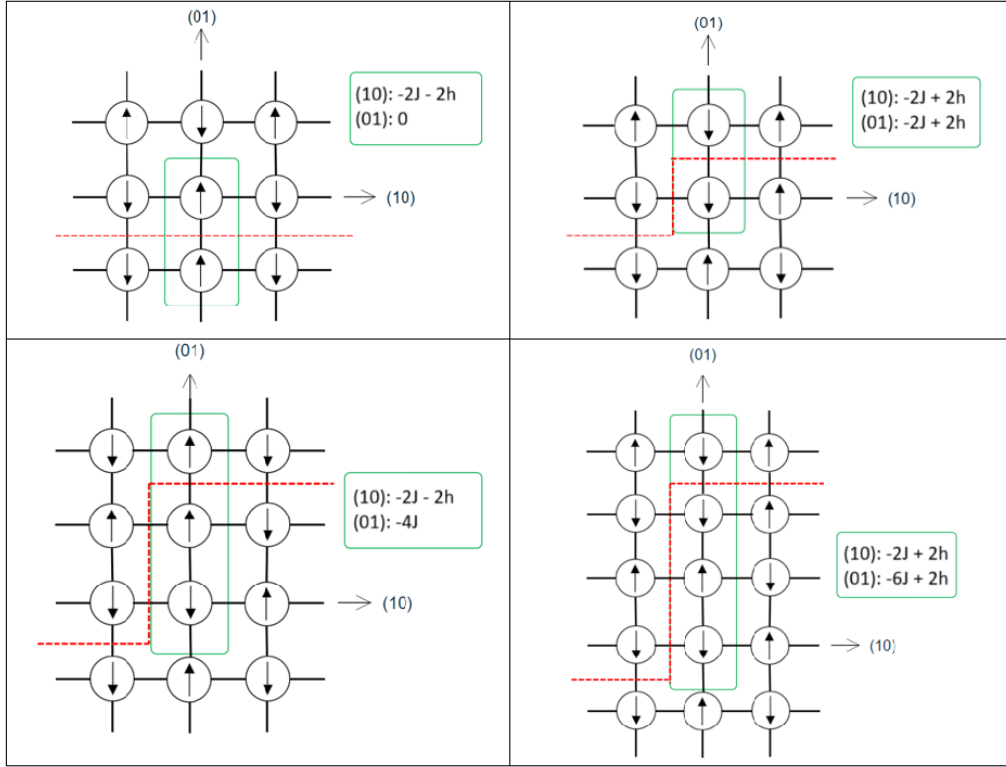


FIGURE 11: Illustration of a boundary segment and three kinks with lengths 1,2 and 3 in the (01)-direction. The green box indicates the spins we consider for the Hamiltonian.

the system. This decreases the free energy of the domain wall since the free energy follows from $F = U - TS$. The formation energy of a kink is dependent on the length of the kink, n , in the y - or (01)-direction and the magnetic field, so we again need to consider the position of the kink. In figure 11 three kinks are depicted with length $n = 1, 2, 3$ which form *after* a $\downarrow\downarrow$ -pair, here the formation energy in the (10)- and (01)-directions are also shown, these are calculated in the same way as before, this can also be done for a kink after an $\uparrow\uparrow$ -pair. We observe a regularity in the formation energy per unit length of the boundary segment. This is given by equation 25 for a kink after an up-up boundary segment and by equation 26 for a kink after a down-down boundary segment.

$$E_{Kink,\uparrow\uparrow} = -2nJ - h(1 + (-1)^{n+1}) \text{ where } n \in \mathbb{N} \quad (25)$$

$$E_{Kink,\downarrow\downarrow} = -2nJ + h(1 + (-1)^{n+1}) \text{ where } n \in \mathbb{N} \quad (26)$$

A.2 Partition function

With these formation energies for the boundary, we can set up the partition function for the boundary in the (10)-direction going through a $\uparrow\uparrow$ or $\downarrow\downarrow$ pair. We must consider all possible routes to make one step in the (10)-direction. This can be straight on or with a kink of length n in either (01)-direction. This gives the following partition functions:

$$Z_{\uparrow\uparrow} = e^{-(-2J-2h)/k_bT} \left(1 + \frac{1}{2} \cdot 2 \sum_{n=1}^{\infty} e^{-(-2nJ+h(1+(-1)^{n+1}))/k_bT} + \frac{1}{2} \cdot 2 \sum_{n=1}^{\infty} e^{-(-2nJ-h(1+(-1)^{n+1}))/k_bT} \right) \quad (27)$$

and

$$Z_{\downarrow\downarrow} = e^{-(-2J+2h)/k_bT} \left(1 + \frac{1}{2} \cdot 2 \sum_{n=1}^{\infty} e^{-(-2nJ+h(1+(-1)^{n+1}))/k_bT} + \frac{1}{2} \cdot 2 \sum_{n=1}^{\infty} e^{-(-2nJ-h(1+(-1)^{n+1}))/k_bT} \right). \quad (28)$$

The factor 2 in the partition function arises because the boundary can kink both upward and downward [6], as can be seen in figure 1. The factor 1/2 arises because the spin couples point up or down half of the lattice due to the antiferromagnetic ordering [10]. Equations 27 and 28 describe the different possibilities for the boundary to move through the different spin directions. Due to the magnetic field, one direction is energetically more favourable than the other since the formation energy for the $\uparrow\uparrow$ step costs less energy than the $\downarrow\downarrow$ step. Therefore the partition function for the boundary in general will be:

$$Z_{(10)} = Z_{\uparrow\uparrow}^p Z_{\downarrow\downarrow}^{1-p}, \quad (29)$$

here p is the probability that the boundary moves in the $\uparrow\uparrow$ direction. Looking at equations 27 and 28 we see that

$$Z_{\uparrow\uparrow} = e^{4h/k_bT} \cdot Z_{\downarrow\downarrow}. \quad (30)$$

From this it follows that the probability p should be:

$$p = \frac{Z_{\uparrow\uparrow}}{Z_{\uparrow\uparrow} + Z_{\downarrow\downarrow}} = \frac{e^{4h/k_bT}}{e^{4h/k_bT} + 1} = \frac{1}{e^{-4h/k_bT} + 1}. \quad (31)$$

The total partition function of one step in the (10)-direction can then be described by: With these formation energies for the boundary, we can set up the partition function for the boundary in the (10)-direction:

$$Z_{(10)} = \left[e^{-(-2J-2h)/k_bT} \left(1 + \frac{1}{2} \cdot 2 \sum_{n=1}^{\infty} e^{-(-2nJ+h(1+(-1)^{n+1}))/k_bT} + \frac{1}{2} \cdot 2 \sum_{n=1}^{\infty} e^{-(-2nJ-h(1+(-1)^{n+1}))/k_bT} \right) \right]^p \cdot \left[e^{-(-2J+2h)/k_bT} \left(1 + \frac{1}{2} \cdot 2 \sum_{n=1}^{\infty} e^{-(-2nJ+h(1+(-1)^{n+1}))/k_bT} + \frac{1}{2} \cdot 2 \sum_{n=1}^{\infty} e^{-(-2nJ-h(1+(-1)^{n+1}))/k_bT} \right) \right]^{1-p}. \quad (32)$$

The factor 2 in the partition function arises because the boundary can kink both upward and downward [6]. The factor 1/2 arises because the spin couples point either up or down half of the lattice [10].

A.3 Absolute convergence of the infinite series

Within the partition function of equation 32 we observe two infinite series concerning the kinks of the boundary. We want to rewrite these series in a closed form, therefore we would like these series to behave like geometric series. Before we can write down the series as a closed form we must be able to rewrite the series in the partition function so the oscillating term $h(1 + (-1)^{n+1})$ disappears and we can split each series into two geometric series. For this, we want to be able to apply theorem 1 [11] and so we need the series to be absolutely convergent.

This theorem needs that the series are absolutely convergent such that we can split the series into its odd and even terms. To show that the series are absolutely convergent we will prove the following lemma:

Lemma 3 (Absolute convergence of the series). *The series $\sum_{n=1}^{\infty} e^{-(-2nJ+h(1+(-1)^{n+1}))/k_bT}$ and $\sum_{n=1}^{\infty} e^{-(-2nJ-h(1+(-1)^{n+1}))/k_bT}$ are absolutely convergent under the conditions that $J < 0$ and $J < h$.*

Proof. Consider the series $\sum_{n=1}^{\infty} e^{-(-2nJ \pm h(1+(-1)^{n+1}))/k_bT}$. For these series to be absolutely convergent it must hold that $\sum_{n=1}^{\infty} |e^{-(-2nJ \pm h(1+(-1)^{n+1}))/k_bT}| < \infty$.

Notice that

$$\sum_{n=1}^{\infty} |e^{-(-2nJ \pm h(1+(-1)^{n+1}))/k_bT}| = \sum_{n=1}^{\infty} e^{-(-2nJ \pm h(1+(-1)^{n+1}))/k_bT},$$

since $e^x > 0$ for all $x \in \mathbb{R}$.

To show this series is absolutely convergent we will apply the root test [11] as described by theorem 6 in appendix B. For our series, this becomes:

$$r = \limsup_{n \rightarrow \infty} |e^{-(-2nJ \pm h(1+(-1)^{n+1}))/k_bT}|^{1/n} = \limsup_{n \rightarrow \infty} e^{-(-2J \pm \frac{h}{n}(1+(-1)^{n+1}))/k_bT}.$$

We see that as n increases that the expressions $e^{-(-2J \pm \frac{h}{n}(1+(-1)^{n+1}))/k_bT}$ are bounded above, so we can write:

$$e^{-(-2J + \frac{h}{n}(1+(-1)^{n+1}))/k_bT} \leq e^{-(-2J)/k_bT}$$

and

$$e^{-(-2J - \frac{h}{n}(1+(-1)^{n+1}))/k_bT} \leq e^{-(-2J - 2h)/k_bT}.$$

So for the two series, we find:

$$r = e^{-(-2J)/k_bT}$$

and

$$r = e^{-(-2J-2h)/k_b T}.$$

Because $J < 0$ and $J < h$ it follows that $r < 1$ in both cases, hence both series are absolutely convergent. \square

Both of the conditions used in the proof for the absolute convergence already hold by the assumptions of the model, so they are met in our derivation. If the magnetic field would point in the opposite direction the same conditions would still hold due to the symmetry of the two series but each condition would apply to the other series. Because we have proven that both series are absolutely convergent, we may now apply theorem 1 and we find:

$$\begin{aligned} \sum_{n=1}^{\infty} e^{-(-2nJ+h(1+(-1)^{n+1}))/k_b T} &= \sum_{n=1}^{\infty} e^{-(-4nJ)/k_b T} + \sum_{n=1}^{\infty} e^{-(-4nJ+2J+2h)/k_b T} \\ &= \frac{e^{4J/k_b T}}{1 - e^{4J/k_b T}} + \frac{e^{(2J-2h)/k_b T}}{1 - e^{4J/k_b T}} = \frac{e^{4J/k_b T} + e^{(2J-2h)/k_b T}}{1 - e^{4J/k_b T}} \end{aligned}$$

And

$$\begin{aligned} \sum_{n=1}^{\infty} e^{-(-2nJ-h(1+(-1)^{n+1}))/k_b T} &= \sum_{n=1}^{\infty} e^{-(-4nJ)/k_b T} + \sum_{n=1}^{\infty} e^{-(-4nJ+2J-2h)/k_b T} \\ &= \frac{e^{4J/k_b T}}{1 - e^{4J/k_b T}} + \frac{e^{(2J+2h)/k_b T}}{1 - e^{4J/k_b T}} = \frac{e^{4J/k_b T} + e^{(2J+2h)/k_b T}}{1 - e^{4J/k_b T}} \end{aligned}$$

A.4 Phase Boundary Equation

With these results, we can rewrite the partition function of equation 32 as follows:

$$\begin{aligned} Z_{(10)} &= \left[e^{-(-2J-2h)/k_b T} \left(1 + \frac{2e^{4J/k_b T} + e^{(2J+2h)/k_b T} + e^{(2J-2h)/k_b T}}{1 - e^{4J/k_b T}} \right) \right]^p \\ &\cdot \left[e^{-(-2J+2h)/k_b T} \left(1 + \frac{2e^{4J/k_b T} + e^{(2J+2h)/k_b T} + e^{(2J-2h)/k_b T}}{1 - e^{4J/k_b T}} \right) \right]^{1-p}. \end{aligned} \quad (33)$$

With this partition function, we are able to prove the following theorem:

Theorem 5 (Phase Boundary Equation).

The phase boundary equation of the antiferromagnetic two-dimensional square Ising model with isotropic nearest neighbour interaction is given by:

$$e^{(-2J+2h-4ph)/k_b T_c} (1 - e^{4J/k_b T_c}) = 1 + e^{4J/k_b T_c} + e^{(2J+2h)/k_b T_c} + e^{(2J-2h)/k_b T_c}$$

Proof. With the partition function of equation 33 we can calculate the free energy of the system:

$$F_{(10)} = -k_b T \ln(Z_{(10)}) = -2J + 2h - 4ph - k_b T p \ln \left(1 + \frac{2e^{4J/k_b T} + e^{(2J+2h)/k_b T} + e^{(2J-2h)/k_b T}}{1 - e^{4J/k_b T}} \right) - k_b T (1-p) \ln \left(1 + \frac{2e^{4J/k_b T} + e^{(2J+2h)/k_b T} + e^{(2J-2h)/k_b T}}{1 - e^{4J/k_b T}} \right). \quad (34)$$

The critical temperature can be found by setting the domain wall free energy to zero, i.e. $F_{(10)} = 0$. This gives the expression:

$$-2J + 2h - 4ph = k_b T_c p \ln \left(1 + \frac{2e^{4J/k_b T_c} + e^{(2J+2h)/k_b T_c} + e^{(2J-2h)/k_b T_c}}{1 - e^{4J/k_b T_c}} \right) + k_b T_c (1-p) \ln \left(1 + \frac{2e^{4J/k_b T_c} + e^{(2J+2h)/k_b T_c} + e^{(2J-2h)/k_b T_c}}{1 - e^{4J/k_b T_c}} \right). \quad (35)$$

Since the right-hand side is of the form $p \cdot A + (1-p) \cdot A$, we can simplify this to:

$$-2J + 2h - 4ph = k_b T_c \ln \left(1 + \frac{2e^{4J/k_b T_c} + e^{(2J+2h)/k_b T_c} + e^{(2J-2h)/k_b T_c}}{1 - e^{4J/k_b T_c}} \right). \quad (36)$$

This gives the following phase boundary equation:

$$e^{(-2J+2h-4ph)/k_b T_c} (1 - e^{4J/k_b T_c}) = 1 + e^{4J/k_b T_c} + e^{(2J+2h)/k_b T_c} + e^{(2J-2h)/k_b T_c}, \quad (37)$$

where p is still defined as in equation 31. □

A.5 Phase diagram

With the phase boundary equation of equation 37 we can develop the phase diagram of the system, this can be seen in figure 12. This figure also includes the condition that the coupling constant J should be greater than the magnetic field strength h , this is indicated by the dashed lines. In this figure, the magnetic field can point in either the up, $h > 0$, or down $h < 0$ direction, since the same result will be acquired when the direction of h flips. Also, the ferromagnetic alignment condition is included.

In this figure we see a clear antiferromagnetic (AF) region whenever the spin-spin interaction J is strong enough and J is stronger than the magnetic field h . In the vicinity of the Onsager point, i.e. $\frac{J}{k_b T_c} = \frac{1}{2} \ln(\sqrt{2} + 1) \approx 0.4406867\dots$ and $h = 0$, we see that for $J < |h|$ a paramagnetic (P) region occurs. Here the spin-spin interaction is not strong enough to form an antiferromagnetic configuration and the magnetic field is not strong enough to align all the spins into a ferromagnetic (F) configuration. This transition indicates an order-disorder phase transition. Around the condition that $J = |h|$ we see that the system

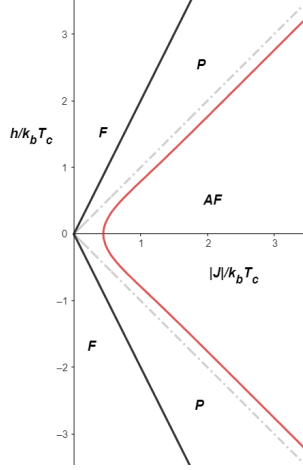


FIGURE 12: Phase diagram of the two-dimensional square Ising model with isotropic nearest neighbour interaction. The red line indicates the critical temperature T_c and the dashed lines indicate whenever $J = h$ or $J = -h$. The black lines indicate the ferromagnetic alignment condition $2|J| < h$ as found in section 2.6.1.

is already in the paramagnetic phase, this implies that the system will transition to the disordered state before the magnetic field is as strong as the spin-spin interaction. This can be attributed to the effect of the temperature since this will also increase the entropy and thus decrease the free energy.

A.6 Vanishing magnetic field

When we consider a vanishing magnetic field in expression 35, i.e. $h \rightarrow 0$ we find:

$$2J = -k_b T_c \ln \left(1 + \frac{2e^{4J/k_b T_c} + 2e^{2J/k_b T_c}}{1 - e^{4J/k_b T_c}} \right)$$

Note that

$$\frac{2e^{2x} + 2e^{4x}}{1 - e^{4x}} = \frac{2e^{2x}(1 + e^{2x})}{(1 - e^{2x})(1 + e^{2x})} = \frac{2e^{2x}}{1 - e^{2x}} \text{ for } x \neq 0.$$

Since $x = J/k_b T_c \neq 0$, we find:

$$2J = -k_b T_c \ln \left(1 + \frac{2e^{2J/k_b T_c}}{1 - e^{2J/k_b T_c}} \right) \quad (38)$$

This is equivalent to Onsager's expression for the Ising model without an external magnetic field with isotropic nearest neighbour interaction in equation 1. This equivalence is proven for the anisotropic case with lemma 2.

B Root test

Theorem 6 (Root test).

Let $a_k \in \mathbb{R}$ and $r := \limsup_{k \rightarrow \infty} |a_k|^{1/k}$.

- i) If $r < 1$, then $\sum_{k=1}^{\infty} a_k$ is absolutely convergent.*
 - ii) If $r = 1$, then the root test is inconclusive.*
 - iii) If $r > 1$, then $\sum_{k=1}^{\infty} a_k$ diverges.*
-